

# Results from MINOS and NO $\nu$ A

**C Backhouse**

California Institute of Technology  
M/C 356-48, 1200 E California Blvd, Pasadena, CA 91125, USA  
E-mail: bckhouse@caltech.edu

**Abstract.**

The MINOS experiment, operating in the NuMI beam since 2005, has provided the most precise measurement of the atmospheric mass splitting  $|\Delta m_{32}^2|$ , and the recent combination of the  $\nu_\mu$ ,  $\nu_e$ , and atmospheric neutrino samples has provided some evidence of non-maximal mixing, and hints about the neutrino mass hierarchy and the  $\theta_{23}$  octant. Construction of the NO $\nu$ A experiment, situated off-axis in the upgraded NuMI beam, is almost complete. Over the coming years it will have significant power to probe the questions of the mass hierarchy,  $\theta_{23}$  octant, and the possibility of  $\mathcal{CP}$  violation in the lepton sector. This paper gives an overview of the results from MINOS, and of the sensitivity of the NO $\nu$ A experiment.

## 1. Introduction

The MINOS and NO $\nu$ A experiments are both situated on the NuMI neutrino beam-line. 120GeV protons from the Fermilab Main Injector strike a graphite target, the resulting pions are focussed by two magnetic horns, and decay to produce a beam of primarily muon neutrinos. Observing the energy-dependent disappearance of these muon neutrinos, and subdominant appearance of electron neutrinos provides information about the neutrino oscillation parameters. Both experiments make use of a two-detector design, in which observations by a Near Detector allow measurements of the beam flux, cross-sections and detector effects, while a larger, but otherwise similarly constructed, Far Detector observes the change in the beam composition over a much longer baseline.

## 2. MINOS

The MINOS detectors are magnetized steel-scintillator tracking sampling calorimeters. They consist of alternating planes of 2.54cm thick steel and 4.1cm $\times$ 1cm solid scintillator strips. Each scintillator strip contains an embedded wavelength-shifting fibre, read out at both ends by Hamamatsu multi-pixel PMTs. Adjacent scintillator planes are oriented at 90 $^\circ$  to each other, allowing for 3D event reconstruction. The detectors are magnetized by a coil to a field of around 1T, allowing for charge identification of muons from curvature.

The MINOS Far Detector is located underground in the Soudan mine, Minnesota, 735km from the NuMI target. It has a total mass of 5.4kton, and has been operating since 2003. The Near Detector is located underground at Fermilab, about 1km downstream from the target. It has a mass of about 1kton, and was completed in 2005. Since 2005, the NuMI beam-line has delivered  $10.7 \times 10^{20}$  protons-on-target (POT) to MINOS in the “low energy” neutrino configuration, and  $3.36 \times 10^{20}$  POT in antineutrino configuration, plus smaller samples in special configurations. In

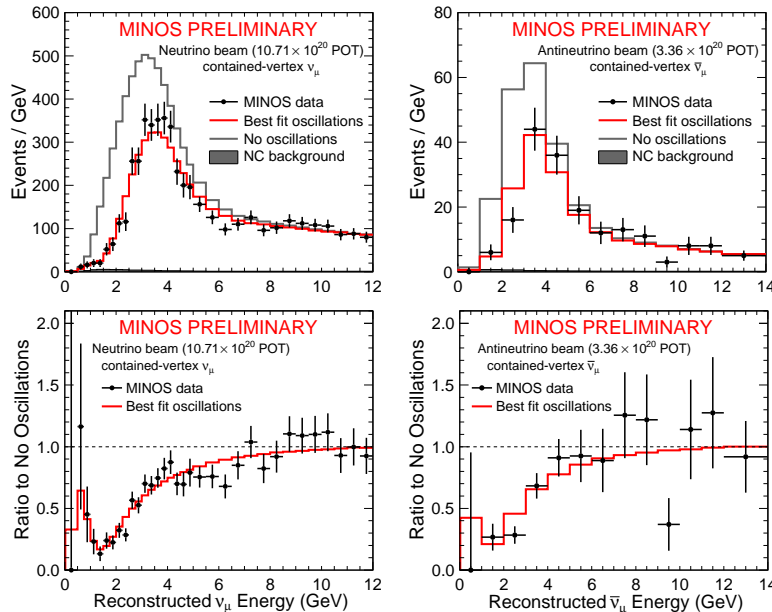


**Figure 1.** Energy spectra from the MINOS neutrino disappearance analyses. The black points are the observed event counts, with statistical errors. The grey curves show the expectation in the absence of oscillations, and the red curves show the best oscillation fit. Agreement with the oscillation hypothesis is very good for both neutrino mode (left) and antineutrino mode (right). The lower panels display ratios to the unoscillated prediction.

addition, MINOS has collected an exposure of 37.8 kton years of atmospheric neutrinos. In 2013, following a shutdown, the NuMI beam returned, delivering neutrinos to NO $\nu$ A (and MINOS+ and MINER $\nu$ A) in the new “medium energy” configuration, optimized to give the greatest flux around oscillation maximum ( $\sim 2\text{GeV}$ ) given NO $\nu$ A’s off-axis location.

Extrapolating from the observed neutrino spectrum in the Near Detector, in the absence of oscillations, MINOS would expect to select 3201  $\nu_\mu$  interactions in the Far Detector, and 363 interactions in the antineutrino running. The observed counts are 2579 and 312 respectively. Figure 1 shows the spectral shapes of these deficits, compared to the best fit from the neutrino oscillation hypothesis. The three-flavour oscillation paradigm fits the data well: 18% of Monte Carlo pseudo-experiments have a worse fit [1].

The inclusion of atmospheric neutrino samples into the analysis provides additional sensitivity, particularly to the mass hierarchy. The unoscillated expectation is for 1100 events, 905 are observed. Figure 2 shows the spectra of the contained muon-selected events as a function of zenith angle. Partially-contained and showering events are also included in the analysis as additional samples.

Selecting electron neutrino candidates, the expectation for  $\theta_{13} = 0$  is 69.1 events of background in neutrino mode, and 10.5 in antineutrinos. The counts observed in data are 88 and 12. Figure 3 shows these excesses in bins of energy and PID value. The hypothesis that  $\theta_{13} = 0$  is rejected at the 96% confidence level [2].

Combining the information provided by the  $\nu_\mu$ , atmospheric, and  $\nu_e$  samples, plus additional constraints on  $\theta_{13}$  from reactor experiments provides some sensitivity to the neutrino hierarchy and  $\theta_{23}$  octant. The solar parameters ( $\Delta m_{21}^2$ ,  $\theta_{12}$ ) are held fixed in this analysis.  $\theta_{13}$  is treated as a nuisance parameter, constrained by external reactor results.  $\delta_{CP}$ ,  $\theta_{23}$ , and  $\Delta m_{32}^2$  are unconstrained and determined by the joint best fit to all the spectra. Major sources of systematic error are included as nuisance parameters.

Figure 4 shows the confidence contours obtained in ( $\Delta m_{32}^2$ ,  $\sin^2 \theta_{23}$ ) space. The best fit value of  $\sin^2 \theta_{23}$  is 0.41, and maximal mixing is disfavoured at 79% confidence. The data also weakly favour the inverted hierarchy and the lower  $\theta_{23}$  octant. Figure 5 shows a different projection of this information, with  $\delta_{CP}$  information included. The most disfavoured scenario is the combination of normal hierarchy and upper  $\theta_{23}$  octant which is rejected at the 81% confidence

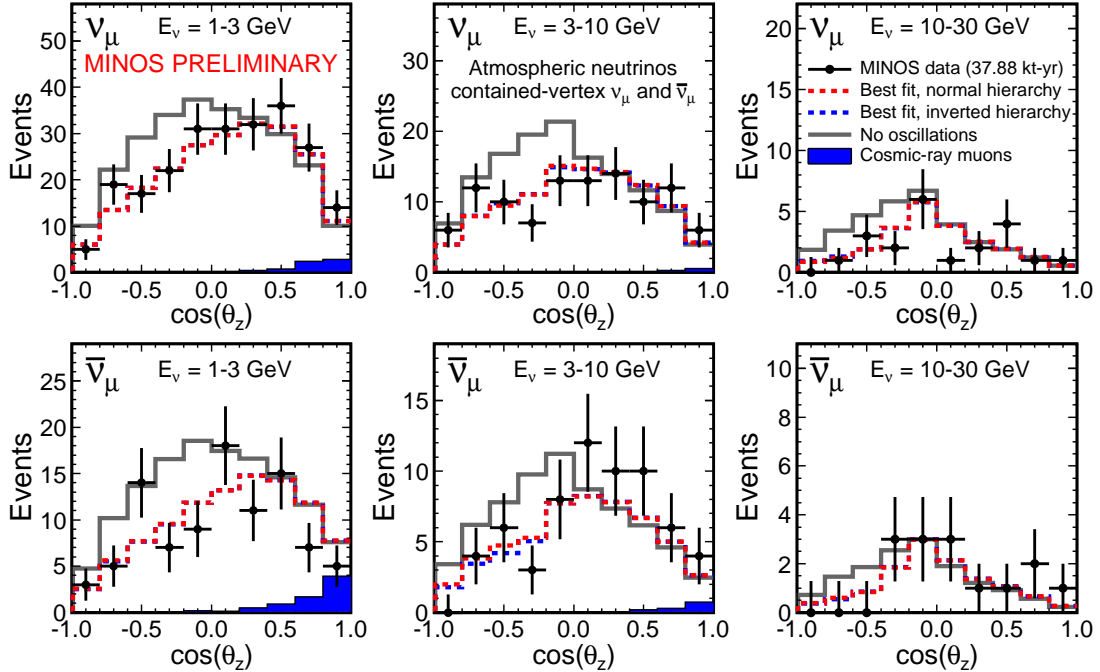


**Figure 2.** Spectra for the MINOS atmospheric neutrino sample. The points show the observed event counts as a function of reconstructed zenith angle. The grey curves show the unoscillated predictions, and the red and blue dashed curves are the best oscillation fits assuming normal or inverted hierarchy respectively. The filled blue histograms indicate the background due to cosmic-ray muons.

**Table 1.** Summary of MINOS combined oscillation fit results for normal and inverted hierarchy.

Parameter	Best fit	Confidence limits (NH)	Best fit	Confidence limits (IH)
$ \Delta m_{32}^2 /10^{-3} \text{eV}^2$	2.37	2.28 - 2.46 (68% C.L.)	2.41	2.32 - 2.53 (68% C.L.)
$\sin^2 \theta_{23}$	0.41	0.35 - 0.65 (90% C.L.)	0.41	0.34 - 0.67 (90% C.L.)

Preference for inverted hierarchy:  $-2\Delta \log L=0.23$

Preference for lower octant:  $-2\Delta \log L=0.09$

Exclusion of maximal mixing:  $-2\Delta \log L=1.54$  ( $\rightarrow$  79% C.L.)

level for all values of  $\delta_{CP}$ . This measurement is also the most precise determination of  $|\Delta m_{32}^2|$ . The results are summarized numerically in Table 1 [3].

If some component of the disappearing MINOS flux were oscillating to sterile neutrinos, one would expect to also see a deficit of neutral current events, in addition to the deficit seen in  $\nu_\mu$  charged currents. In fact, a search for this effect found a small excess of neutral current interactions at the Far Detector as compared to predictions. Interpreting in terms of oscillations around  $\Delta m^2 \sim 0.5 \text{eV}^2$  leads to a limit  $\sin^2 2\theta_{\mu e} < 7.1 \times 10^{-3}$  at the 90% confidence level.

The MINOS detectors continue to operate in the NO $\nu$ A-era beam. The higher energy peak of the neutrino flux reduces the statistics acquired in the oscillation region, but the statistics at higher energies are greatly increased. MINOS+ expects to collect around 4,000  $\nu_\mu$  charged current events per year. This high-statistics sample will allow tests of the standard three-flavour oscillation paradigm, including searches for sterile neutrinos, and sensitivity to signatures of

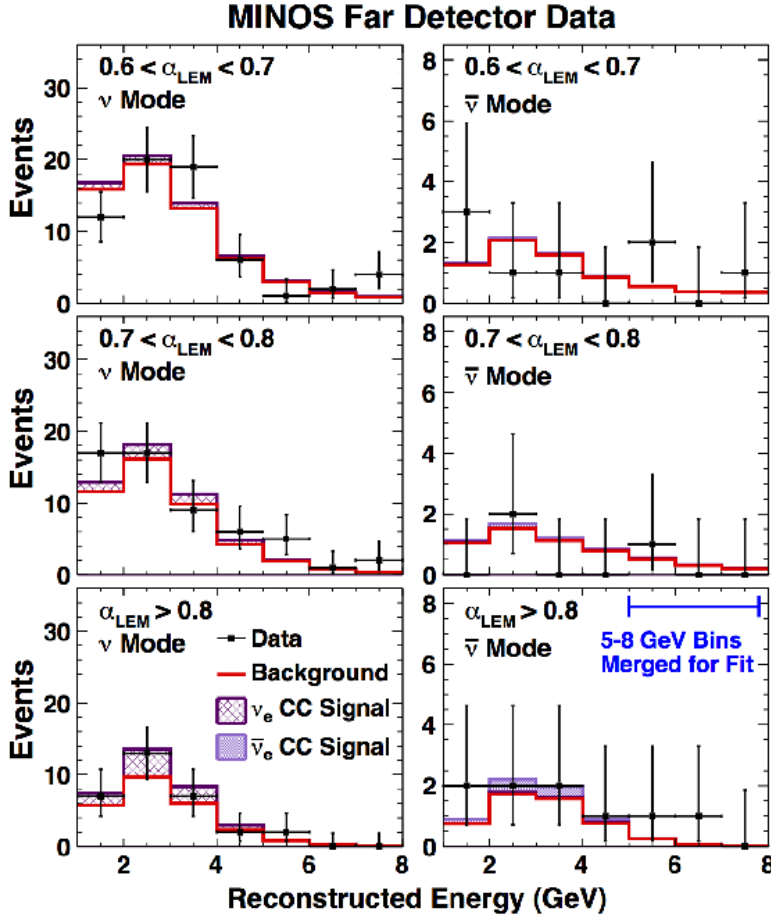


**Figure 3.** Spectra of  $\nu_e$ -selected events in MINOS. The points are the number of events selected as a function of reconstructed neutrino energy. The red curve shows the prediction for  $\theta_{13} = 0$ , and the purple region shows the excess for the best-fit value of  $\theta_{13}$ . The samples are divided by PID value (top to bottom) and between neutrino (left) and antineutrino (right) running. The data is divided into bins of PID value, from the lowest selected PIDs (top) to the most  $\nu_e$ -like events (bottom). 88 neutrino-mode events and 12 antineutrino-mode events are selected, compared to an expectation for  $\theta_{13} = 0$  of 69.1 and 10.5. The expectations for  $\theta_{13} = 0.1$  are 95.1 and 13.6.

exotic physics such as large extra dimensions.

### 3. NO $\nu$ A

The NO $\nu$ A detectors are fine-grained, low-Z, highly active tracking calorimeters. Cells of extruded PVC, approximately  $6\text{cm} \times 4\text{cm}$  are formed into planes, with the orientation of successive planes alternating as in MINOS. They are filled with a mineral oil/liquid scintillator mix, which comprises 64% of the detector by mass. Each cell contains a looped wavelength-shifting fibre, read out at one end by one of the 32 pixels of a Hamamatsu avalanche photodiode (APD), cooled to  $-15^\circ\text{C}$  [4].

The Far Detector is located on the surface at Ash River, Minnesota, 810km from the NuMI target. The detector consists of 344,000 channels, approximately  $16 \times 16 \times 60\text{m}$ , for a total mass of 14kton. Assembly and placement of the plastic blocks, scintillator filling, and electronics installation proceed in parallel. All blocks are now in place, and oil filling is almost complete. Over 2/3 of the detector is instrumented with APDs and being read out. The Near Detector is located underground at Fermilab, approximately 1km from the target. It comprises 18,000 channels, with a mass of 0.3kton. All blocks are in place, and oil filling and electronics outfitting are in progress. The NuMI beam is being upgraded from a maximum capacity of 350kW up to 700kW. This will be achieved by converting the Recycler from running antiprotons to protons, and shortening the cycle in the Main Injector from 2.2s to 1.33s. The beam has been running stably since returning from shutdown in September 2013, and power is gradually being increased. The maximum power achievable will be limited to 500kW until upgrading of the Booster RF

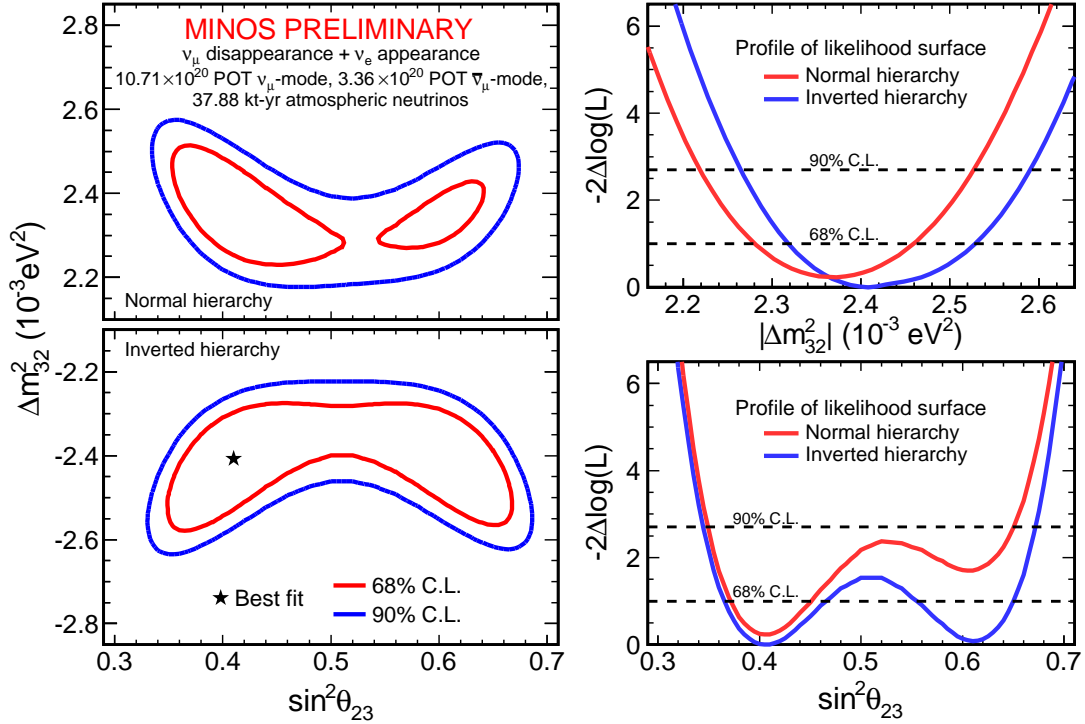


**Figure 4.** Combined results from the MINOS  $\nu_\mu$ ,  $\nu_e$ , and atmospheric analyses. The star shows the best fit values of  $\sin^2 \theta_{23}$  and  $\Delta m_{32}^2$ . This point weakly favours non-maximal mixing, the lower octant, and inverted hierarchy. The red and blue contours indicate 68% and 90% confidence levels. The panels on the right display the profile likelihood projection onto each of the two parameters.

cavities is complete. Thus far, in excess of  $1.5 \times 10^{20}$  protons have been delivered.

It is important to validate the detectors' ability to pick neutrino interactions out of the cosmic-ray background, and to verify the synchronization of the Far Detector to the NuMI spill times. Analysis of the Near Detector prototype on the surface at Fermilab (NDOS) shows a clear peak in the neutrino candidate timing spectrum over the cosmic-ray background. Propagating this timing information to the Far Detector gives a  $10\mu\text{s}$  window in which neutrinos are expected to be found. A combination of automated analysis and hand-scanning of events in a  $500\mu\text{s}$  window around this point (plus out-of-time spills for background estimation) found four candidate events within the timing window, on a background of 0.05. The times of the events relative to the beam window were kept secret until after the choice of these events had been finalized. Figure 7 shows the NDOS timing peak compared to the times of the selected neutrino candidates, and Figure 8 shows one of the Far Detector events in the timing window, a multi-pronged interaction, with reconstructed neutrino direction coming from Fermilab.

The sensitivity projections presented below assume  $18 \times 10^{20}$  POT of data taken in neutrino mode plus  $18 \times 10^{20}$  POT taken with antineutrinos. This corresponds to a nominal  $6 \times 10^{20}$  POT per year and a run plan with three years in each mode. The choice of what exposure to take in each beam configuration is flexible, and may be adjusted in response to changing circumstances. The oscillation parameters assumed are  $\sin^2 2\theta_{13} = 0.095$   $\sin^2 2\theta_{23} = 0.95$  or 1.0 depending on context. We take  $\Delta m_{32}^2 = 2.35 \times 10^{-3} \text{eV}^2$ , and the other parameters from the latest Particle Data Group averages [5].

Current global constraints on the atmospheric mixing angle are around  $\sin^2 2\theta_{23} \gtrsim 0.9$ ,

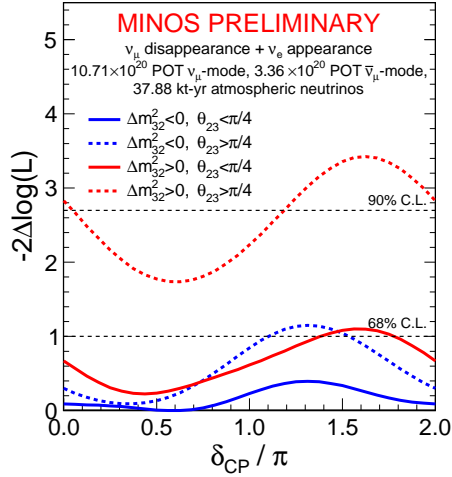


**Figure 5.** Log-likelihood differences from the best fit oscillation parameters for different values of  $\delta_{CP}$ , hierarchy and  $\theta_{23}$  octant for the combination of MINOS analyses. The region normal hierarchy, upper octant,  $\delta_{CP} \sim \frac{3\pi}{2}$  is disfavoured at greater than 90% confidence.

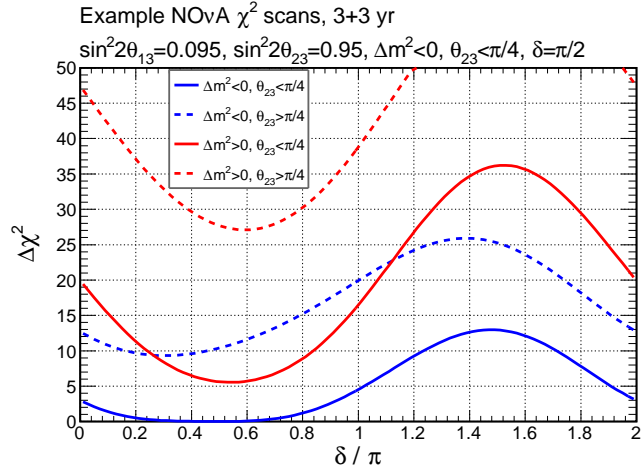


**Figure 6.** Sensitivity of NO $\nu$ A for a nominal run of three years neutrino plus three antineutrino ( $18 \times 10^{20}$  POT each). The true oscillation values are chosen to be close to the MINOS best-fit. The shape of the curves is very similar to the MINOS results in Figure 5, but the expected sensitivity is much higher. For example, the most disfavoured scenario, normal hierarchy, upper octant, would be excluded at  $5\sigma$  for all values of  $\delta_{CP}$ .

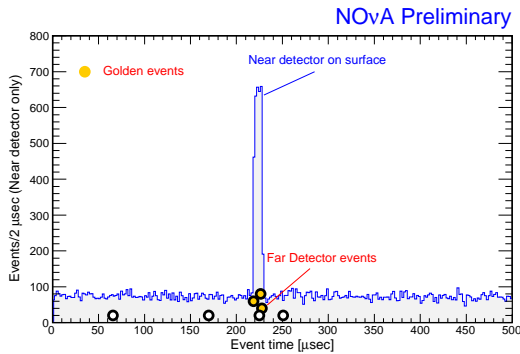


**Figure 7.** The timing peak formed by neutrinos from the NuMI beam in the NDOS detector (filled histogram) with the times of selected interactions in the NO $\nu$ A Far Detector marked (circles). The Far Detector events were found by a combination of hand-scanning and automated analysis. The estimated cosmic-ray background in the  $10\mu\text{s}$  Far Detector spill window is 0.05 events.

with hints of non-maximal mixing from MINOS. The NO $\nu$ A experiment will have significantly enhanced power to distinguish between maximal and non-maximal mixing. The  $\nu_\mu$  charged current analysis being developed separates the data into three samples: quasi-elastic candidates, which are very pure with good energy reconstruction; the remainder of contained candidates; and uncontained events, where the muon exits through the back or side of the detector, a sample with substantial statistics, but poor energy resolution. Predicted event counts are given in Table 2. The contours that would be obtained with increasing exposure are shown in Figure 9, for two possible values of  $\theta_{23}$ . With three years of neutrino running, and three years of antineutrinos, this analysis should obtain percent-level uncertainty on the atmospheric mixing parameters. If  $\sin^2 \theta_{23} = 0.95$ , maximal mixing could be excluded at 90% confidence with one year of running.

Table 2 also shows the representative event counts for the sample of electron neutrino candidates. As with MINOS, sensitivity to the mass hierarchy,  $\theta_{23}$  octant, and  $\delta_{CP}$  comes from combining the disappearance and appearance analyses, plus constraints on  $\theta_{13}$  from reactor

**Figure 8.** Event display of the first neutrino candidate event selected in the NO $\nu$ A Far Detector. Each square represents energy deposited and detected in a single cell. The neutrino beam enters from the left. The top panel shows the information from vertically-oriented cells, with horizontal cells shown in the bottom panel. The overlaid coloured lines are the reconstructed paths of particles, and the cross marks the reconstructed position of the interaction vertex.

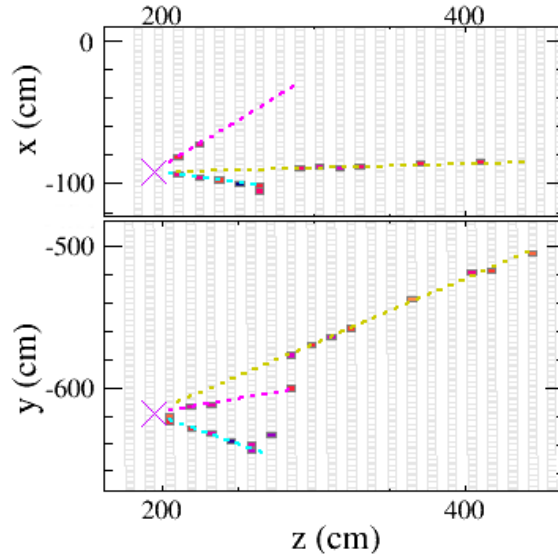


**Table 2.** Representative event counts for NO $\nu$ A analyses. The columns represent  $18 \times 10^{20}$  POT neutrino-mode and antineutrino-mode running. The  $\nu_\mu$  analysis divides the dataset into three samples, candidate quasielastic events, non-quasielastic events, and events where the muon is not fully contained within the detector. The counts are constrained to the range 0-5GeV, the region of sensitivity to oscillations driven by the atmospheric mass splitting.

$\nu_e$ selected	$\nu$	$\bar{\nu}$
NC	19	10
$\nu_\mu$ CC	5	< 1
Beam $\nu_e$	8	5
Tot bkg	32	15
Signal	68	32

$\nu_\mu$ selected	$\nu_\mu$ CC	NC	$\bar{\nu}_\mu$ CC	NC
Quasielastic	82	< 1	49	< 1
non-QE	168	14	78	6
Uncontained	233	6	134	3

(0-5GeV visible energy)

experiments. Figure 10 shows the sensitivity of this analysis to these three parameters, as a function of the true values of  $\delta_{CP}$  and the mass hierarchy. For the mass hierarchy, there are degenerate regions where it is not possible to disentangle the matter effects, which give information about the mass hierarchy, from true  $\mathcal{CP}$ -violation driven by  $\delta_{CP}$ . But for favourable combinations  $2 - 3\sigma$  evidence for the mass hierarchy can be obtained. Determination of the  $\theta_{23}$  octant is much less sensitive to  $\delta_{CP}$  and can be achieved at better than  $2\sigma$  for all values of  $\delta_{CP}$  if  $\sin^2 2\theta_{23} = 0.95$ . The lower octant is assumed in order to match the best fit from MINOS, performance for the upper octant is slightly better. Figure 6 shows predicted  $\Delta\chi^2$  slices as a function of  $\delta_{CP}$ , to be compared with the analogous Figure 5 from MINOS data. The true parameters are chosen to match the MINOS best fit (inverted hierarchy, lower octant,  $\delta_{CP} \sim \frac{\pi}{2}$ ).

**Figure 9.** Projected 90% confidence contours in the  $(\Delta m_{32}^2, \sin^2 \theta_{23})$  space for two, six, or ten years of running (assuming  $6 \times 10^{20}$  POT per year), for two values of  $\theta_{23}$ . In the case of  $\sin^2 2\theta_{23} = 0.95$ , maximal mixing can be excluded at 90% confidence in under two years of running.

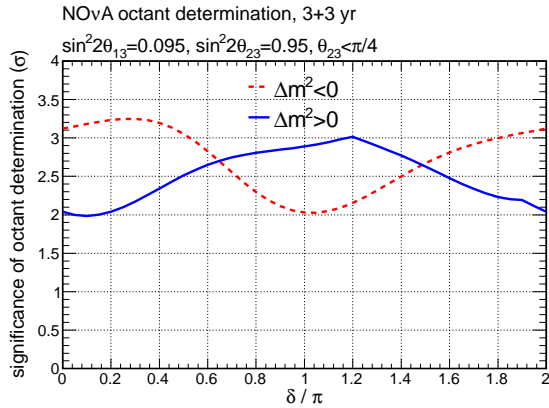
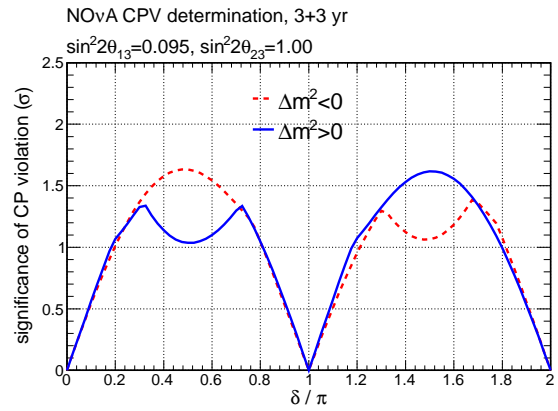
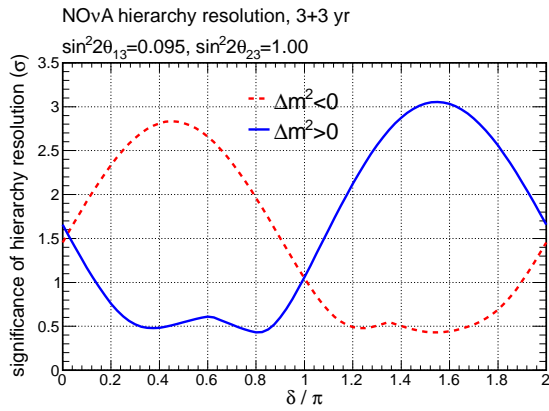
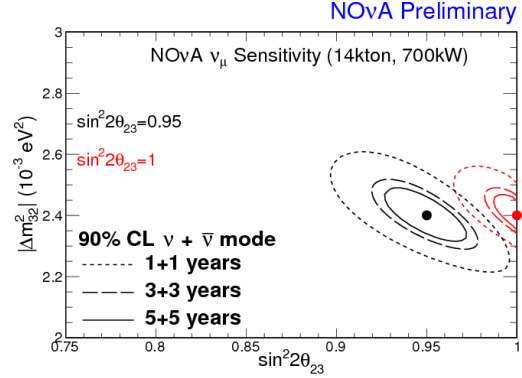


**Figure 10.** Sensitivity of NO $\nu$ A to resolve the mass hierarchy (top left), discover  $\mathcal{CP}$  violation (above), and resolve the  $\theta_{23}$  octant (left) as a function of the true value of  $\delta_{CP}$ . The solid blue curves are in the case that the true mass hierarchy is normal, the dashed red curves are for the inverted case. In each case,  $\sin^2 2\theta_{13} = 0.095$  is assumed. For hierarchy and  $\mathcal{CP}$  violation  $\sin^2 2\theta_{23} = 1$  is assumed, the octant sensitivity assumes  $\sin^2 2\theta_{23} = 0.95$ , first octant.

If the true parameters are indeed in this region, NO $\nu$ A would reject parts of phase space (in particular the combination of normal hierarchy and upper octant) at very high significance.

#### 4. Conclusion

The MINOS experiment has collected a large sample of neutrino interactions in over six years of running, in both neutrino and antineutrino mode. A combined fit to this data gives the world's most precise measurement of  $|\Delta m_{32}^2|$ , and hints for the neutrino mass hierarchy and  $\theta_{23}$  octant. These detectors will continue taking data in the NO $\nu$ A-era beam as MINOS+.

Construction of the NO $\nu$ A experiment is progressing well. First neutrinos have been found in the Far Detector, and projections show good sensitivity to the mass hierarchy and  $\theta_{23}$  octant, in addition to improved measurements of the atmospheric mixing parameters. Results from the next few years, in combination with other experiments, should provide significant information

on these questions for the first time.

## References

- [1] Adamson P *et al.* 2013 *Phys. Rev. Lett.* **110**, 251801
- [2] Adamson P *et al.* 2013 *Phys. Rev. Lett.* **110**, 171801
- [3] Adamson P *et al.* 2014 *Preprint* hep-ex/1403.0867, submitted to *Phys. Rev. Lett.*
- [4] Ayres D S *et al.* 2007 FERMILAB-DESIGN-2007-01
- [5] Beringer J *et al.* 2012 *Phys. Rev. D* **86**, 010001